




Metabolism of synthetic cathinones through the zebrafish water tank model: a promising tool for forensic toxicology laboratories

Estefany Prado¹ · Rebecca Rodrigues Matos¹ · Geovana Maria de Lima Gomes¹ · Clarisse Baptista Lima de Sá¹ · Isabelle Karine da Costa Nunes¹ · Carina de Souza Anselmo¹ · Adriana Sousa de Oliveira² · Luciana Silva do Amaral Cohen² · Denilson Soares de Siqueira² · Marco Antônio Martins de Oliveira^{2,4} · João Carlos Laboissiere Ambrosio³ · Gabriela Vanini Costa^{1,5} · Francisco Radler de Aquino Neto¹ · Monica Costa Padilha¹ · Henrique Marcelo Gualberto Pereira¹ 

Received: 20 May 2020 / Accepted: 8 July 2020 / Published online: 22 July 2020
© The Author(s) 2020

Abstract

Purpose The aim of this study was to identify *in vivo* phase I metabolites of five psychoactive substances: *N*-ethylpentylone, ethylone, methylone, α -PVP and 4-CDC, using the in house developed experimental set-up zebrafish (*Danio rerio*) water tank (ZWT). High-resolution mass spectrometry allowed for metabolite identification. A pilot study of reference standard collection of *N*-ethylpentylone from the water tank was conducted.

Methods ZWT consisted in 8 fish placed in a 200 mL recipient-containing water for a single cathinone. Experiments were performed in triplicate. Water tank samples were collected after 8 h and pretreated through solid-phase extraction. Separation and accurate-mass spectra of metabolites were obtained using liquid chromatography–high resolution tandem mass spectrometry.

Results Phase I metabolites of α -PVP were identified, which were formed involving ketone reduction, hydroxylation, and 2''-oxo-pyrrolidine formation. The lactam derivative was the major metabolite observed for α -PVP in ZWT. *N*-Ethylpentylone and ethylone were transformed into phase I metabolites involving reduction, hydroxylation, and dealkylation. 4-CDC was transformed into phase I metabolites, reported for the first time, involving *N*-dealkylation, *N,N*-bis-dealkylation and reduction of the ketone group, the last one being the most intense after 8 h of the experiment.

Conclusions ZWT model indicated to be very useful to study the metabolism of the synthetic cathinones, such as *N*-ethylpentylone, ethylone, α -PVP and 4-CDC. Methylone seems to be a potent CYP450 inhibitor in zebrafish. More experiments are needed to better evaluate this issue. Finally, this approach was quite simple, straightforward, extremely low cost, and fast for “human-like” metabolic studies of synthetic cathinones.

Keywords Synthetic cathinones · Zebrafish · *In vivo* metabolism · High-resolution mass spectrometry · Human-like experimental model · Reference standard collection in zebrafish water tank

Introduction

The recent advances in analytical instrumentation allowed the development of extremely sensitive and comprehensive drug detection methods [1]. However, these analytical

approaches do not make the modern forensic toxicology a challenge less field. One of the most critical aspects in this area is the vertiginous increase of new substances available in the illegal market around the world [2], which brings a number of relevant new targets for forensics laboratories [3–5].

The class of synthetic cathinones is a remarkable example of this scenario. These compounds are closely related to the naturally occurring cathinone ((*S*)-2-amino-1-phenyl-1-propanone), a β -ketone amphetamine analogue and the main psychoactive compound in the leaves of Khat plant (*Catha edulis*) [6, 7]. The press alerted about them in 2007

Electronic supplementary material The online version of this article (<https://doi.org/10.1007/s11419-020-00543-w>) contains supplementary material, which is available to authorized users.

✉ Henrique Marcelo Gualberto Pereira
henriquemarcelo@iq.ufrj.br

Extended author information available on the last page of the article

[6], and in 2019 they were listed in the top three groups of new psychoactive substances (NPS) seized around the world, just behind of the synthetic cannabinoids and ketamine [8]. This remarkable increase may be related to the fact that a substance once prohibited or tracked down by forensic laboratories is easily replaced in the market by new chemically related analogs after minor structural modifications. In addition, they pose a public health threat as their pharmacological, toxicological and analytical data are usually not available [2–5, 7, 9].

From the methodologic point of view, when the analytical work involves the detection of the abuse of a new substance in biological matrices, the knowledge of drug metabolism becomes essential to define suitable analytical targets. Inevitably, it is necessary to consider the ethical bottleneck to conduct studies in humans without a clear understanding of the drug's toxicology. In this way, alternative models have been used to circumvent the use of human volunteers in metabolism studies [10–12]. Among them, zebrafish (*Danio rerio*) has already demonstrated advantages over in vitro and classical animal models [13–15].

The experimental design so-called “zebrafish water tank” (ZWT) model [13, 15–18] showed success to qualitatively reproduce the human metabolism of xenobiotics from different classes of substances such as anabolic steroids, cannabinimimetics, stimulants and narcotics. These results may be explained by the remarkable enzymatic machinery orthology between the zebrafish and humans [15]. The model allows very simple and robust metabolism experiments using adult zebrafish considering their more complete and mature enzymatic system as compared with the experimental designs using embryos [18, 19]. For the best of our knowledge, no work evaluating if zebrafish is able to mimic the human metabolism of synthetic cathinones can be found in the literature. Considering its experimental simplicity and high throughput, we used ZWT to investigate the metabolism of the cathinones *N*-ethylpentylone, ethylone, methylone, α -pyrrolidinopentiophenone (α -PVP) and 4-chloro-*N,N*-dimethylcathinone (4-CDC) (Fig. 1).

Thus, with the astonishing speed of the appearance of new cathinones, obviously, reference standards of the metabolites are hardly commercially available, which increases the degree of complexity in the characterization of the abuse of these substances in routine forensic toxicology laboratories. Thus, motivated by the lack of reference standards of cathinone metabolites in most forensic laboratories, we developed a pilot study to generate a reference collection based on the ZWT model using the cathinone *N*-ethylpentylone as a model. The results obtained are reported in this work.

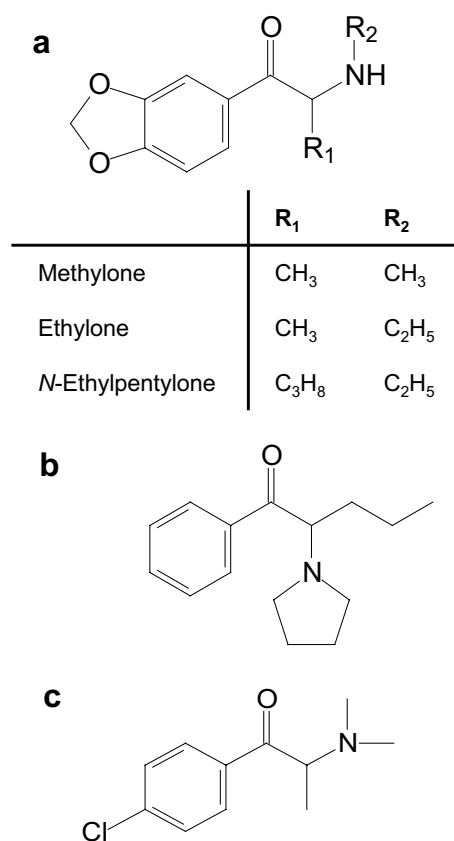


Fig. 1 Chemical structure of **a** 3,4-methylenedioxy-*N*-alkylated cathinones and its R₁, R₂ substitutions. **b** *N*-Pyrrolidine cathinone, α -PVP. **c** *N*-Alkylated cathinone 4-chloro-*N,N*-dimethylcathinone (4-CDC)

Materials and methods

Material and reagents

N-Ethylpentylone, ethylone, methylone, α -PVP and 4-CDC were provided by Brazilian Police Agencies from seized materials on the illicit drug market. Formic acid, acetic acid, ammonium formate, sodium phosphate, acetonitrile, and methanol were of analytical or HPLC grade purchased from Tedia (Fairfield, OH, USA); β -glucuronidase from *E. coli* from Roche (Rio de Janeiro, Brazil); ultrapure water (18 MW cm⁻¹) from Milli-Q Millipore water system (Burlington, MA, USA); Strata-X-CW, weak cation mixed-mode polymeric sorbent (30 mg) solid-phase extraction (SPE) cartridges from Phenomenex (São Paulo, Brazil); D₂O at 99.9% from Cambridge Isotope Laboratory (Andover, MA, USA).

Analysis of the seized products

All cathinones used in the ZWT metabolism study were previously and exhaustively characterized for their

identification and purity using ^1H nuclear magnetic resonance (NMR) spectroscopy, infrared (IR) spectroscopy, liquid chromatography–high-resolution mass spectrometry (LC–HR–MS) (direct flow injection) and gas chromatography–mass spectrometry (GC–MS).

^1H NMR spectroscopy

Approximately 10 mg of each crystal was dissolved in 0.5 mL of D_2O containing 20 ppm of trimethylsilylpropanoic acid (TSP) used as an internal standard. The NMR spectra were recorded using 400 MHz apparatus (Bruker, Bremen, Germany) with D_2O at 99.9% as a solvent. All spectra were acquired at 35 °C. The peak in 4.7 ppm was referenced to the residual water (HOD) suppressed by pre-saturation. The ^1H NMR spectra (Zgpr from Bruker Library) were obtained with 16 scans using a delay between each scan of 1.2 s. The chemical shifts were corrected in relation to the internal standard (TSP) at 0 ppm to the ^1H . All data were processed using TopSpin 3.1 software (Bruker).

IR analysis

The IR spectra of each compound were obtained using a Spectrum Two Fourier-transform infrared (FT-IR) Perkin Elmer[®] Spectrometer (Perkin Elmer, Waltham, MA, USA) with a diamond to achieve attenuated total reflection. Each sample was directly loaded onto the FT-IR instrument and each spectrum was acquired in single mode, with a resolution of 4 cm^{-1} , in the region from 4000 to 550 cm^{-1} and recorded with an average of 4 scans.

GC–MS analysis

For GC–MS system, the samples were prepared using 100 mg of each sample dissolved in 2 mL of methanol (HPLC grade). An aliquot of 20 μL of this solution was diluted with 980 μL of methanol. GC–MS analyses were performed using an Agilent Technologies 6890 N gas chromatograph coupled to an Agilent Technologies model 5973 mass spectrometer (Agilent Technologies, Palo Alto, CA, USA). The injector was maintained at 280 °C. Sample injection (1 μL) was in the splitless mode. Separation of sample components was conducted using the HP-5MS column (Agilent Technologies) with 5% phenyl-95% methylsiloxane (30 m \times 0.25 mm i.d., film thickness 0.25 μm). Helium (99.995% purity) was used as a carrier gas at a constant pressure of 10 psi. The GC oven was held at 50 °C for 1 min, then ramped up at 20 °C min^{-1} to 300 °C and held for 2 min. The mass detector was set to positive electron ionization (EI) mode and the electron beam energy was 70 eV.

The full MS scan mode was acquired in the mass range from m/z 40 to 600.

Maintenance of zebrafish and zebrafish water tank (ZWT) experimental set-up

Acclimation of zebrafish

Adult zebrafish of mixed sex (3–5 months) were used. The fish were obtained from a local provider and acclimatized to groundwater for at least 5 days prior to experimentation in tanks with circulatory pumps. Fish were kept at a temperature of 28 ± 2 °C in a photoperiod of 12:12 h. The fish were fed twice a day with TetraMin[®] ration (Tetra, Blacksburg, VA, USA) during the acclimation process. One day prior to experimentation, feeding was stopped, and the fish were transferred to the test tanks and allowed to rest.

Scale-down of ZWT set up for accumulation curve elaboration

The experiments were performed in 200 mL glass tanks fitted with a heating device set to a temperature of 32 ± 0.5 °C as follows: (1) positive control: without fish and with the single drug previously diluted in water; (2) negative control: without any cathinones and with eight fish; (3) test tanks: with each drug and eight fish. Each cathinone was diluted in water to give a final concentration of $0.5\text{ }\mu\text{g mL}^{-1}$. Aliquots were collected from all tanks at the following times: 0, 0.5, 1, 2, 3, 4, 5, 6, 7 and 8 h of each experiment. The fish were not fed during the experiments.

Scale-up for reference standard collection of *N*-ethylpentylone

The ZWT model was conducted as described by De Souza Anselmo et al. [17] with adaptation. Eighteen adult zebrafish were kept in 4 L aerated water tanks, at 28 ± 2 °C and were fed TetraMin[®] ration once a day during all experiment. One milligram aliquot of *N*-ethylpentylone previously dissolved in water was added to the tank. After 72 h (when the target metabolite concentration was highest), the whole volume of the tank was stored at 4 ± 1 °C and concentrated as described below for elaboration of the reference standard collection.

Sample preparation procedure

Aliquots from the water tank were used as samples. For the elaboration of the accumulation curve, the preparation started at 2 different aliquots. The first of 10 μL tank water was kept at 4 °C to be used below, while the second of the sample was prepared as follows: to 2.5 mL of the water tank, 10 μL of a mixture of internal standard working solutions

was added to obtain a final concentration of 40 ng mL^{-1} each of 7-propyltheophylline, bupirone, and cathine- D_3 ; 5 ng mL^{-1} each of growth hormone-releasing peptide-4- D_4 and testosterone- D_3 ; 4 ng mL^{-1} of JWH-018- D_{11} ; 100 ng mL^{-1} of mefruside and 20 ng mL^{-1} of morphine glucuronide- D_3 . This internal standard mixture solution is used in routine screening procedures in the Brazilian Doping Control Laboratory, where each compound is intended to check a specific step in the overall procedure as described by Sardela et al. [1]. Then, after $75 \mu\text{L}$ of β -glucuronidase from *E. coli* were added, the samples were vortexed, incubated at $50 \pm 1 \text{ }^\circ\text{C}$ for 1 h and cooled to room temperature. Strata-X-CW (30 mg) SPE columns were used in the clean-up/concentration step. The SPE cartridges were inserted into a vacuum manifold and conditioned with 2 mL methanol and 2 mL of ultrapure water. The hydrolyzed samples were applied to the cartridges, washed with 2 mL of ultrapure water, 1 mL of methanol/water (1:1, v/v) and analytes were eluted with 3 mL of methanol/formic acid (95:5, v/v). The eluates were evaporated to dryness under a stream of nitrogen in a $40 \pm 1 \text{ }^\circ\text{C}$ water bath, reconstituted with $50 \mu\text{L}$ of 5% acetic acid and added to the $10 \mu\text{L}$ aliquot previously separated. Then, $8 \mu\text{L}$ were subjected to instrumental analyses.

For the reference standard collection, 200 mL aliquots were added to the cartridges previously conditioned as described above and washed with 2 mL of methanol/water (1:1, v/v). Then, the analytes were eluted with 6 mL of methanol/formic acid (95:5, v/v) and evaporated to dryness under a stream of nitrogen in a $(40 \pm 1) \text{ }^\circ\text{C}$ water bath. The concentrated metabolites mixture was reconstituted in 1 mL of methanol.

Liquid chromatography and mass spectrometry setup

An Accela liquid chromatography (LC) system (Thermo Fisher Scientific, Bremen, Germany) coupled to a Q-Exactive Plus Orbitrap high-resolution mass spectrometer (Thermo Fisher Scientific) was used. The chromatographic separation was performed in a reversed-phase column (SynchronisTM C_{18} , $50 \times 2.1 \text{ mm i.d.}$, particle size $1.7 \mu\text{m}$; Thermo Fisher Scientific, Waltham, MA, USA) with the oven set at $40 \text{ }^\circ\text{C}$. The mobile phases were composed of (A) 5.0 mM ammonium formate water solution and (B) methanol; both phases contained 0.1% formic acid. The flow rate was set at $400 \mu\text{L min}^{-1}$. The elution program was 0–0.3 min, 5% B; 0.3–0.5 min, 5–10% B; 0.5–1.0 min, 10–25% B; 1.0–6.0 min, 25–90% B; 6.0–8.0 min, 90–100% B; 8.0–9.0 min, 100% B (column washing); 9.0–9.1 min, 100–5% B, 9.1–11.0 min, 5% B (column equilibration to the initial condition). The overall run time was 11 min. The LC effluent was pumped to a Q-Exactive mass spectrometer operating in positive ionization mode and equipped with an electrospray ionization

(ESI (+)) source. The spray voltage was set to 3.9 kV; capillary temperature to $380 \text{ }^\circ\text{C}$; and the S-lens radio frequency level to 80 (arbitrary units). The nitrogen sheath and auxiliary gas flow rates were set at 60 and 20 (arbitrary units), respectively. The instrument was calibrated using the manufacturer's calibration solutions (Thermo Fisher Scientific) to ensure mass accuracies below 6 ppm. The mass spectrometer acquired full scan data at a resolution of 70,000 full widths at half maximum (FWHM) and with automatic gain control of 10^6 . Simultaneously, an all-ion fragmentation full scan experiment was also performed in positive ionization mode with a normalized collision energy at 40 and a resolution at 17,500 FWHM. In addition, the cathinones and their metabolites were fragmented and analyzed through data-independent acquisition experiments in the second stage of tandem mass spectrometry (full-scan/ MS^2) at a resolution of 17,500 FWHM, loop count at 5, isolation window at m/z 1.0 and with normalized collision energy (NCE) optimized for each cathinone and metabolite.

Results

Characterization of seized drugs

In GC–MS analysis only one intense chromatographic peak was observed for each sample of synthetic cathinones (Figs. S1 – S3). The mass spectrum of *N*-alkylated cathinones showed an immonium ion as the base peak, formed by an amine initiated α -cleavage, at m/z 58, 72 and 100 ($\text{C}_n\text{H}_{2n+2}\text{N}^+$) for methylone ($n=3$) (Fig. S1a), ethylone ($n=4$) (Fig. S1b) and *N*-ethylpentylone ($n=6$) (Fig. S2a), respectively. A characteristic ion at m/z 121 [$\text{C}_7\text{H}_5\text{O}_2$]⁺, which indicated the presence of the methylenedioxy group attached to an aromatic ring, and the ion at m/z 149 [$\text{C}_8\text{H}_5\text{O}_3$]⁺, corresponding to the addition of the β -keto group to the above structure, was detected in mass spectra of ethylone, methylone and *N*-ethylpentylone (Figs. S1, S2).

The base peak ion at m/z 126 ($\text{C}_8\text{H}_{16}\text{N}^+$) was observed for pyrrolidyl substituted cathinone as α -PVP (Fig. S2b). In addition, an ion at m/z 105 [$\text{C}_7\text{H}_5\text{O}$]⁺ corresponding to the β -keto group attached to the aromatic ring. 4-CDC (Fig. S3a) presented a base peak at m/z 72 corresponding to the *N*-alkyl chain from α -carbonyl cleavage. The mass spectra of cathinones corresponded the spectra in the mass spectra library (SWGDRUG, Software Version: 3.4).

FT-IR spectra obtained from the crystal samples of cathinones were compared with those found in the literature [4] or the equipment Library (SWGDRUG IR Library-version 1.8). A high similarity was verified for each cathinone analyzed. The functional groups of cathinones were displayed in the spectra as the carbonyl stretching conjugated with a phenyl group showing a characteristic absorption at 1673 cm^{-1}

(ethylone, Fig. S1b), 1675 cm^{-1} (methylone, Fig. S1a), 1681 cm^{-1} (*N*-ethylpentylone, Fig. S2a; α -PVP, Fig. S2b) and 1689 cm^{-1} (4-CDC, Fig. S3b).

Regarding the ^1H NMR spectra, the 1,3,4-substituted aromatic ring showed signal H-2, H-5 and H-6 at 7.48, 7.05 and 7.71 ppm, respectively, indicating two doublets and one doublet of doublets. Methylone (Fig. S1a), ethylone (Fig. S1b) and *N*-ethylpentylone (Fig. S2a) presented a signal at 6.14 ppm, corresponding to the methylenedioxy group. The chemical shifts of the units attached to position 1 of the aromatic ring were evaluated for identification purpose. In the methylone sample, two major signals at 2.8 and 1.63 ppm attributed to CH_3 groups were observed (Fig. S1a). A singlet at 1.63 ppm attributed to a CH_3 group bonded to α -carbonyl, and a singlet at 1.43 ppm attributed to protons from CH_3 of the amine-linked ethyl group, were found in the ethylone sample (Fig. S1b). Regarding *N*-ethylpentylone sample, two major signals at 1.37 and 0.88 ppm were observed. The signal at 1.37 ppm corresponded to the protons from CH_3 signal of the amine-linked ethyl group (Fig. S2a). The signal at 0.88 ppm corresponded to the protons of CH_3 of the propyl group bonded to carbon alpha carbonyl. 4-CDC spectrum (Fig. S3c) shows five signals at 7.99 and 7.63 ppm corresponding to the protons H-2 and H-3 from aromatic ring 4-substituted by chlorine. This observation excluded the presence of position isomers (*ortho* and *meta*). The quadruplet signal at 5.13 ppm corresponded to alpha carbonyl proton. At 3.00 and 1.66 ppm would be proton signals from dimethyl amine-linked group and methyl bonded to α -carbonyl, respectively. α -PVP spectrum sample showed a typical phenyl pattern at 7.68, 7.84 and 8.08 ppm (H-3, H-4 and H-2, respectively) (Fig. S2b), and the signals at 5.26 ppm confirmed the structure as α -pyrrolidinopentiophenone. The pyrrolidine proton signals were found at 3.12, 3.73, 3.44 and 2.23 ppm (H-6a, H-6b, H-9 and H-7, respectively). The signals at 0.84, 1.24 and 2.11 ppm corresponded to pentane chain chemical shifts (H-5, H10 and H-8, respectively).

Metabolic studies through ZWT

After the addition of the synthetic cathinones to the tanks, no phenotype modifications or abnormal behavior were observed in the fish. However, it is important to highlight that phenotype observations were not the goal of the study in ZWT, and no detailed observation protocols were in place during the study. However, all fish survived until the end of the experiments, being afterwards treated following the guidance of the ethical protocol in place.

The chemical formulae of the cathinones and respective metabolites found in ZWT as well as the collision energies employed for their fragmentation, retention times (t_R), measured mass to charge ratio for the protonated molecules

and product ions and mass error (ppm) are summarized in Tables 1, 2 and 3 for α -PVP, ethylone and *N*-ethylpentylone, 4-CDC, respectively. The elemental composition obtained from product ion and neutral losses aided the assignment of the structure of metabolites.

α -PVP

In the ZWT experiment, α -PVP was metabolized extensively into five phase I metabolites. Figure 2a shows the proposed metabolic pathways of α -PVP in ZWT (⊙), in vitro studies (⌘) [20], and human urine (⌘) [21]. HR-MS/MS spectra of α -PVP and its hydroxylated metabolite at pyrrolidine ring (M2), β -ketone reduced metabolite (M4) and 2''-oxo pyrrolidine metabolite (M5) are depicted in Fig. 2b. The HR-MS/MS spectra of *N*-dealkylated (M1) and dihydroxylated (M3) metabolites are shown in supplementary material (Fig. S4a).

The HR-MS/MS spectra of α -PVP showed a m/z 161.09604 corresponding to the loss of amine moiety followed by an alkyl chain loss at m/z 119.04936 (Fig. 2b). The benzoyl ion and the immonium cation could be also observed at m/z 105.03381 and 126.12788, respectively. Moreover, m/z 91.05468 could be observed as a base peak due to its high thermodynamic stability [22], although it is not specific for structural elucidation of this compound or its metabolites.

N,N-Bis-dealkyl- α -PVP (M1), formed from a transformation of the pyrrolidine ring into a primary amine, was also observed in in vitro studies [20, 23] but not in human urine [21]. In ZWT, the HR-MS/MS spectra of this metabolite (Fig. S4a) showed specific product ions corresponding to the loss of the keto moiety at m/z 160.11230 followed by the loss of a propyl side chain at m/z 118.06551 and m/z 130.06496 besides the ion also observed at m/z 105.03400 in α -PVP. The result of hydroxylation of the pyrrolidine ring (M2) was observed as a product of diastereomers in humans [21]. In contrast, it was not described for human liver microsome (HLM) [20]. In ZWT, it was observed only one chromatographic peak, the HR-M/MS spectrum of which is shown in Fig. 2b. The specific ions at m/z 230.15450 and 142.12267 correspond to the loss of hydroxy group as water and the immonium cation with the addition of the hydroxy group, respectively. It also showed a peak at m/z 161.09619 corresponding to the loss of hydroxylated amine moiety and benzoyl ion at m/z 105.03387. It is noteworthy that the position of the hydroxylation in the pyrrolidine ring could not be assessed by means of LC–HR-MS; therefore, it was represented by tilde. Dihydroxylated derivative (M3) (Fig. S4a) was observed in in vitro studies [20, 23], but was not identified in humans [21]. HR-MS/MS spectra showed a loss of water at m/z 232.16985 and 214.15927 followed by the loss of propyl chain at m/z 172.11227.

Table 1 Putative identification of in vivo metabolites of α -PVP using the zebrafish water tank (ZWT) model in the presence of 5 ng mL⁻¹ of α -PVP after 8 h analyzed by liquid chromatography–high-resolution tandem mass spectrometry (LC–HR-MS/MS)

α -PVP or metabolites	Metabolic reaction	Formula [M+H] ⁺	Measured product ion (<i>m/z</i>)	Mass error (ppm)	NCE (eV)	Product ion formulae	Measured product ions (<i>m/z</i>)	Mass errors (ppm)	<i>t_R</i> (min)
α -PVP	–	C ₁₅ H ₂₂ NO	232.16946	0.43	50	C ₁₁ H ₁₃ O ⁺	161.09604	0.31	4.48
						C ₈ H ₁₆ N ⁺	126.12788	1.27	
						C ₈ H ₇ O ⁺	119.04936	1.85	
						C ₇ H ₅ O ⁺	105.03381	3.05	
						C ₇ H ₇ ⁺	91.05468	5.00	
M1	<i>N,N</i> -Bis-dealkylation	C ₁₁ H ₁₆ NO	178.12294	1.68	50	C ₁₁ H ₁₄ N ⁺	160.11230	1.40	4.25
						C ₉ H ₈ N ⁺	130.06496	1.27	
						C ₈ H ₈ N ⁺	118.06551	3.25	
						C ₇ H ₅ O ⁺	105.03400	4.80	
M2	Hydroxylation in the pyrrolidine ring	C ₁₅ H ₂₂ NO ₂	248.6440	0.42	50	C ₁₅ H ₂₀ ON ⁺	230.15454	2.06	4.35
						C ₁₁ H ₁₃ O ⁺	161.09619	0.61	
						C ₈ H ₁₆ NO ⁺	142.12267	0.21	
						C ₇ H ₅ O ⁺	105.03387	3.60	
M3	Dihydroxylation	C ₁₅ H ₂₄ NO ₂	250.18040	0.98	50	C ₁₅ H ₂₂ ON ⁺	232.16985	1.12	4.50
						C ₁₅ H ₂₀ N ⁺	214.15927	1.14	
						C ₁₁ H ₁₄ N ⁺	160.11226	1.12	
						C ₁₂ H ₁₄ N ⁺	172.11227	1.13	
M4	β -Ketone reduction	C ₁₅ H ₂₄ NO	234.18535	0.47	50	C ₁₅ H ₂₂ N ⁺	216.17456	0.24	4.59
						C ₁₂ H ₁₅ N ⁺	173.12003	0.74	
						C ₁₁ H ₁₃ ⁺	145.10123	0.36	
M5	Hydroxylation + dehydrogenation	C ₁₅ H ₂₀ NO ₂	246.14897	0.49	45	C ₁₅ H ₁₈ ON ⁺	228.13840	0.48	6.79
						C ₁₁ H ₁₃ O ⁺	161.09616	0.42	
						C ₁₁ H ₁₁ ⁺	143.08566	0.93	
						C ₈ H ₁₄ ON ⁺	140.10709	0.71	
						C ₇ H ₅ O ⁺	105.03392	4.08	

NCE normalized collision energy, *t_R* retention time

1-Hydroxy- α -PVP (**M4**), presented a loss of water at *m/z* 216.17445, followed by a propyl side chain loss as a radical cation at *m/z* 173.11980, or pyrrolidine ring loss at *m/z* 145.10106 (Fig. 2b). 2''-Oxo- α -PVP (**M5**), product of hydroxylation followed by dehydrogenation in the pyrrolidine ring, was also observed in human urine [21]. This metabolite was not observed in in vitro studies, i.e., HLM [20]. In the MS² spectrum for ZWT the loss of water yielding *m/z* 228.13840 could be observed, as well as the loss of a keto benzyl moiety at *m/z* 143.08566 and *m/z* 140.10709.

The results of the ZWT has as complementary evidence for the accumulation profile of the α -PVP metabolites through time, as presented in Fig. S4b. For α -PVP, 1-hydroxy- α -PVP (**M4**) presented the most significative accumulation profile, followed by **M5** and **M2**. At the end of the 8 h of experiments, the major metabolic pathway identified for α -PVP in ZWT, i.e., the most accumulated metabolite, was the reduction of the β -ketone to give an alcohol, **M4**.

N-Ethylpentylone and ethylone

As *N*-ethylpentylone and ethylone are structurally similar, it is not unsurprising that comparable metabolic pathways have been observed in ZWT. The phase I metabolic pathways observed for *N*-ethylpentylone are common to ethylone and are presented in Fig. 3a. Metabolites could be observed resulting from keto reduction (**M1**), hydroxylation in alkyl chain (**M2**) and demethylenation (**M3**) in ZWT after 8 h of experiment. Chemical formula of *N*-ethylpentylone, ethylone and their three metabolites and their respective product ions, NCE employed for their fragmentation, retention time (*t_R*), measured *m/z* for the protonated molecules and product ions, and mass error (ppm) are summarized in Table 2.

Loss of water from the hydroxy group was observed as a base peak at *m/z* 234.14986 for *N*-ethylpentylone metabolite (**M1**) and at *m/z* 206.10789 Da for ethylone. Hydroxylation of *N*-ethylpentylone and ethylone resulted in the formation of **M2**,

Table 2 Putative identification of in vivo metabolites of *N*-ethylpentylone or ethylone using the ZWT model in the presence of 5 ng mL⁻¹ of either drug after 8 h analyzed by LC–HR–MS/MS

Parent or metabolite	Metabolic reaction	Formula [M + H] ⁺	Measured <i>m/z</i>	Mass error (ppm)	<i>t_R</i> (min)	NCE	Product ion formula	Product ion <i>m/z</i>	Mass errors (ppm)	<i>t_R</i> (min)	NCE (eV)	Product ion formula	Product ion <i>m/z</i>	Mass errors (ppm)		
<i>N</i> -Ethylpentylone	–	C ₁₄ H ₁₉ NO ₃	250.14468	3.64	4.25	25	C ₁₄ H ₁₈ NO ₂ ⁺	232.13405	1.27	3.65	40	C ₁₂ H ₁₄ NO ₂ ⁺	204.10274	4.11		
			252.16045	4.08	4.14	25	C ₁₂ H ₁₃ O ₃ ⁺	205.08667	0.98				C ₁₁ H ₁₂ NO ⁺	174.09210	4.36	
			252.16045	4.08	4.14	25	C ₁₃ H ₁₆ NO ⁺	202.12340	1.04					C ₉ H ₇ O ₂ ⁺	147.04468	4.62
M1	β-Ketone reduction	C ₁₄ H ₂₁ NO ₃	252.16045	4.08	4.14	25	C ₈ H ₁₄ N ⁺	100.11279	1.65				C ₁₂ H ₁₆ NO ₂ ⁺	206.10789	2.49	
			252.16045	4.08	4.14	25	C ₁₄ H ₂₀ NO ₂ ⁺	234.14986	1.65					C ₁₁ H ₁₄ NO ⁺	176.09766	3.52
			252.16045	4.08	4.14	25	C ₁₂ H ₁₅ O ₃ ⁺	207.10246	1.95					C ₁₂ H ₁₆ NO ₂ ⁺	206.10789	2.49
M2	Hydroxylation on the alkyl chain	C ₁₄ H ₁₉ NO ₄	266.13770	3.68	4.82	25	C ₁₃ H ₁₆ NO ⁺	202.12349	1.49				C ₁₂ H ₁₅ NO ₃	224.12802	2.90	
			266.13770	3.68	4.82	25	C ₆ H ₁₄ N ⁺	100.11287	2.45					C ₁₂ H ₁₅ NO ₄	238.10800	2.58
			266.13770	3.68	4.82	25	C ₁₄ H ₁₈ NO ₃ ⁺	248.12932	2.62					C ₁₂ H ₁₄ O ₃ N ⁺	220.09700	0.82
M3	Demethylation	C ₁₃ H ₁₅ NO ₃	238.14496	5.00	3.59	25	C ₁₂ H ₁₃ O ₄ ⁺	221.08182	2.62				C ₁₁ H ₁₂ O ₂ N ⁺	190.08626	0.05	
			238.14496	5.00	3.59	25	C ₆ H ₁₄ N ⁺	100.11279	1.65					C ₁₁ H ₁₄ O ₂ N ⁺	192.10184	0.34
			238.14496	5.00	3.59	25	C ₁₃ H ₁₆ NO ⁺	220.13425	2.25					C ₁₁ H ₁₂ ON ⁺	174.09142	0.46

1-(1,3-benzodioxol-5-yl)-2-(ethylamino)-hydroxy-pentan-1-one and 1-(1,3-benzodioxol-4-ol-5-yl)-2-(ethylamino)-hydroxy-propan-1-one, respectively (Fig. 3b). **M2** exhibited protonated ions at *m/z* 266.13770 for *N*-ethylpentylone and at *m/z* 238.10800 for ethylone. The position of hydroxylation along the alkyl chain for these metabolites could not be determined by mass spectrometry experiments. In Fig. 3a the unknown position is demonstrated by tilde. Demethylation of *N*-ethylpentylone and ethylone generated **M3**, 1-(3,4-dihydroxyphenyl)-2-(ethylamino)pentan-1-one and 1-(3,4-dihydroxyphenyl)-2-(ethylamino)propan-1-one, respectively (Fig. 3b). **M3** exhibited a protonated ion of at *m/z* 238.14496 for *N*-ethylpentylone and at *m/z* 210.11243 for ethylone.

4-Chloro-*N,N*-dimethylcathinone

In ZWT, a reduced metabolite (**M1**, *m/z* 214.09932), nor-metabolite *N*-dealkylated (**M2**, *m/z* 198.06802) and bis-nor-metabolite (**M3**, *m/z* 184.05236) were detected. Figure 4a presents the HR-MS/MS spectra of the putative metabolites observed in ZWT after 8 h of experiment. All ion fragmentation acquisition mode in the LC–HR-MS system allowed the detection of the expected chlorine cluster shared by all chlorinated metabolites (Fig. 4b). HR-MS/MS spectra were obtained using data-independent acquisition mode with a narrow isolation window of *m/z* 1.0 despite the loss of the isotopic information for the sake of sensitivity. Chemical formula of 4-CDC, its metabolites and their respective product ions, NCE employed for fragmentation, retention time (*t_R*), measured mass to charge ratio for the protonated molecules and product ions, and mass error (ppm) are summarized in Table 3.

4-CDC presented the loss of the amino moiety at *m/z* 167.02591 as base peak and the formation of a benzoyl ion at *m/z* 139.03096 in its HR-MS/MS spectrum (Fig. 4a). The protonated-molecular ion and product ion at *m/z* 139.03096 presented the isotope pattern expected for ³⁵Cl/³⁷Cl (Fig. 4b). Xcalibur 3.0 program was used to calculate the theoretical isotope distribution for the chlorine group of 4-CDC and its metabolites. Furthermore, the isotope intensity for [M + H]⁺ and the product ions (Fig. 4b) were also performed in three other ZWT samples collected after 8 h of the experiment. The all ion fragmentation scan analysis for this mass was repeated 3 times for every sample and compared with the theoretical intensity.

As described by Niessen and Correa [24], loss of water (– 18.0106 Da, H₂O) is characteristic of the fragmentation pattern of cathinones, but not pyrrolidinophenones. This neutral loss was observed as a base peak in **M1**, product of reduction on the keto moiety (*m/z* 196.08885) (Fig. 4a). The consecutive loss of CH₃ yielded a peak at *m/z* 181.06537. **M2** and **M3**, products of *N*-dealkylation and

Table 3 Putative identification of in vivo metabolites of 4-CDC using the ZWT model in the presence of 5 ng mL⁻¹ of 4-chloro-*N,N*-dimethylcathinone (4-CDC) after 8 h analyzed by LC–HR-MS/MS

4-CDC Metabolite	Metabolic reaction	Formula	Measured <i>m/z</i>	Mass error (ppm)	NCE (eV)	Product ion formulae	Product ions (<i>m/z</i>)	Mass errors (ppm)	<i>t_R</i> (min)
4-CDC	–	C ₁₁ H ₁₅ NOCl	212.08369	0.14	40	C ₉ H ₈ ClO ⁺ C ₇ H ₄ ClO ⁺	167.02591 139.03096	0.54 0.40	4.22
M1	β-Ketone reduction	C ₁₁ H ₁₇ NOCl	214.09920	0.55	35	C ₁₁ H ₁₅ NCl ⁺ C ₁₀ H ₁₂ NCl ⁺	198.08875 181.06537	0.49 0.50	4.04
M2	<i>N</i> -Dealkylation	C ₁₀ H ₁₃ NOCl	198.06807	0.11	40	C ₁₀ H ₁₁ NCl ⁺ C ₉ H ₈ OCi ⁺ C ₁₀ H ₁₁ N ⁺	180.05745 167.02589 145.08859	0.02 0.42 0.07	4.06
M3	<i>N</i> -Bis-dealkylation	C ₉ H ₁₁ NOCl	184.05257	1.10	35	C ₉ H ₉ NCl ⁺ C ₉ H ₉ N ⁺	166.04193 131.07317	0.76 1.67	3.98

N,N-bis-dealkylation, showed the loss of the keto group at *m/z* 180.05745 and 166.04193 for **M2** and **M3**, respectively (Fig. 4a). The loss of the amino moiety yielded a peak at *m/z* 167.02589 for **M2**. Both metabolites (**M2** and **M3**) showed the loss of a chlorine group at *m/z* 145.08859 and 131.07317, respectively. The proposed metabolic route is shown in Fig. 5a.

In ZWT, after 8 h of the experiment the product of reduction of the keto group of 4-CDC (**M1**) was the most intense metabolite and *N*-demethylation (**M2**) the second most intense (Fig. 5b). None of these metabolites were found in the negative (with fish without drug) and positive (with the drug without fish) controls.

Methylone

First described as an NPS in 2005, methylone (2-methylamino-1-(3,4-methylenedioxyphenyl)propan-1-one) was raised in Japan and Europe [25–27] in the early 2000's. Originally synthesized as an anti-Parkinsonism agent [27], this drug received the street-name “Explosion”, mainly in Europe. Kamata et al. [26] investigated methylone metabolism through both human and rat models reporting two major metabolic pathways. The *N*-demethylation to the corresponding primary amine methylenedioxcathinone was characterized generating metabolite. Demethylation, followed by *O*-methylation of either a 3- or 4-OH group on the benzene ring to produce 4-hydroxy-3-methoxymethcathinone, took place, and the isomer 3-hydroxy-4-methoxymethcathinone were also observed in free and conjugated forms. None of these metabolites was previously reported in the literature observed through the ZWT experiment. Indeed, despite the use of very sensitive analytical approaches, no other molecular entity similarly related to methylone could be detected in the tanks, indicating that all metabolite process was inhibited. The whole of methylone is considered as inhibitor of CYP isoforms.

Reference standard collection

N-Ethylpentylone was chosen as a model substance to the reference standard collection experiment considering the extensive metabolism data available in the literature and apparently, in Brazil, but no metabolites of *N*-ethylpentylone are not commercially available at this time; we may have the high prevalence of this synthetic cathinone. SPE was chosen as a concentration strategy considering its practicality and availability in toxicology laboratories. Moreover, SPE can provide additional clean up, eliminating undesirable particles such as animal excrement and feed scraps. Thus, the metabolites were biosynthesized by 18 fish, and after 72 h, 20 aliquots of 200 mL of water were eluted in 10 preconditioned SPE cartridges. The metabolites were recovered with methanol/formic acid (95:5, v/v) solution. A rough estimation of concentration was performed by the ratio between the chromatographic peak area of each metabolite and that of the internal standard 7-propyltheophylline. Thus, it could be observed that metabolite concentrations increased approximately 100-folds, when compared with the original aquarium water sample.

Such a procedure allowed the detection of all metabolites in the previously scale down experiment. The methanolic solution was shared with the Brazilian Police Forces (DGPTC/PCERJ and SEPLAB) to support their own toxicologic laboratories. The reference standard collection was also distributed to the WADA Laboratories community allowing the implementation of *N*-ethylpentylone in their own routines. This reference standard collection pilot study showed that this kind of material can be produced very fast and with low cost, becoming a very straightforward tool for forensic toxicology laboratories.

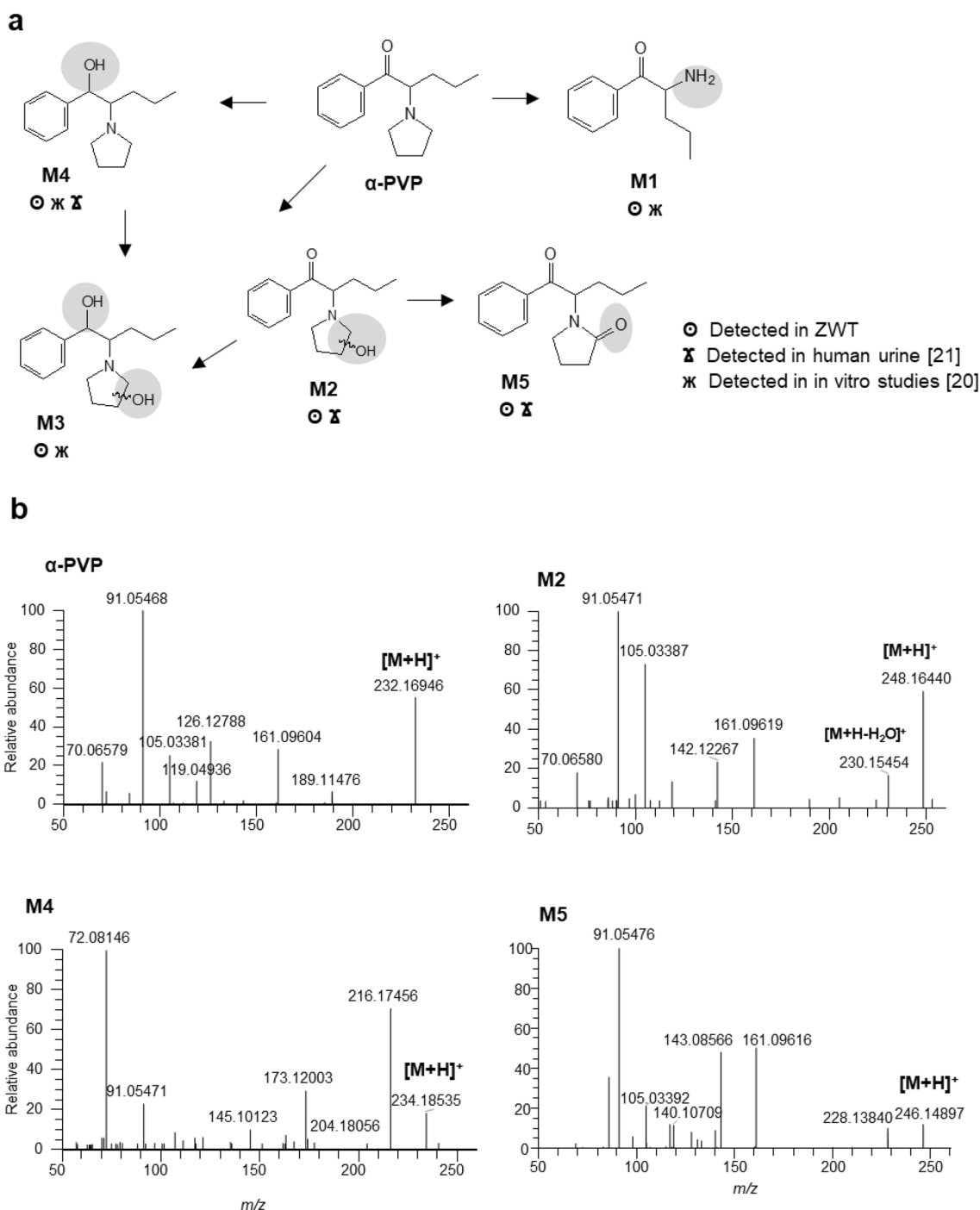


Fig. 2 a Proposed in vivo metabolic pathways for α -PVP based on metabolites observed in zebrafish water tank (ZWT); unclear position of the hydroxy group represented by special marks; metabolic reac-

tions highlighted in grey in each structure. **b** High-resolution tandem mass (HR-MS/MS) spectra with electrospray ionization (ESI(+)) of α -PVP, M2 M4 and M5 obtained from the water in ZWT

Discussion

All five cathinones used in the metabolic studies were the result of apprehension by the Brazilian security forces. As typically observed in South American countries, the most common substances available on the drug market in Brazil

were those from plant-based sources, e.g., cocaine and cannabis. This may be justified by the intense production of these drugs in the continent, especially in the neighboring countries [8, 28]. Nevertheless, considering that all materials used in this study came from the Brazilian illegal market,

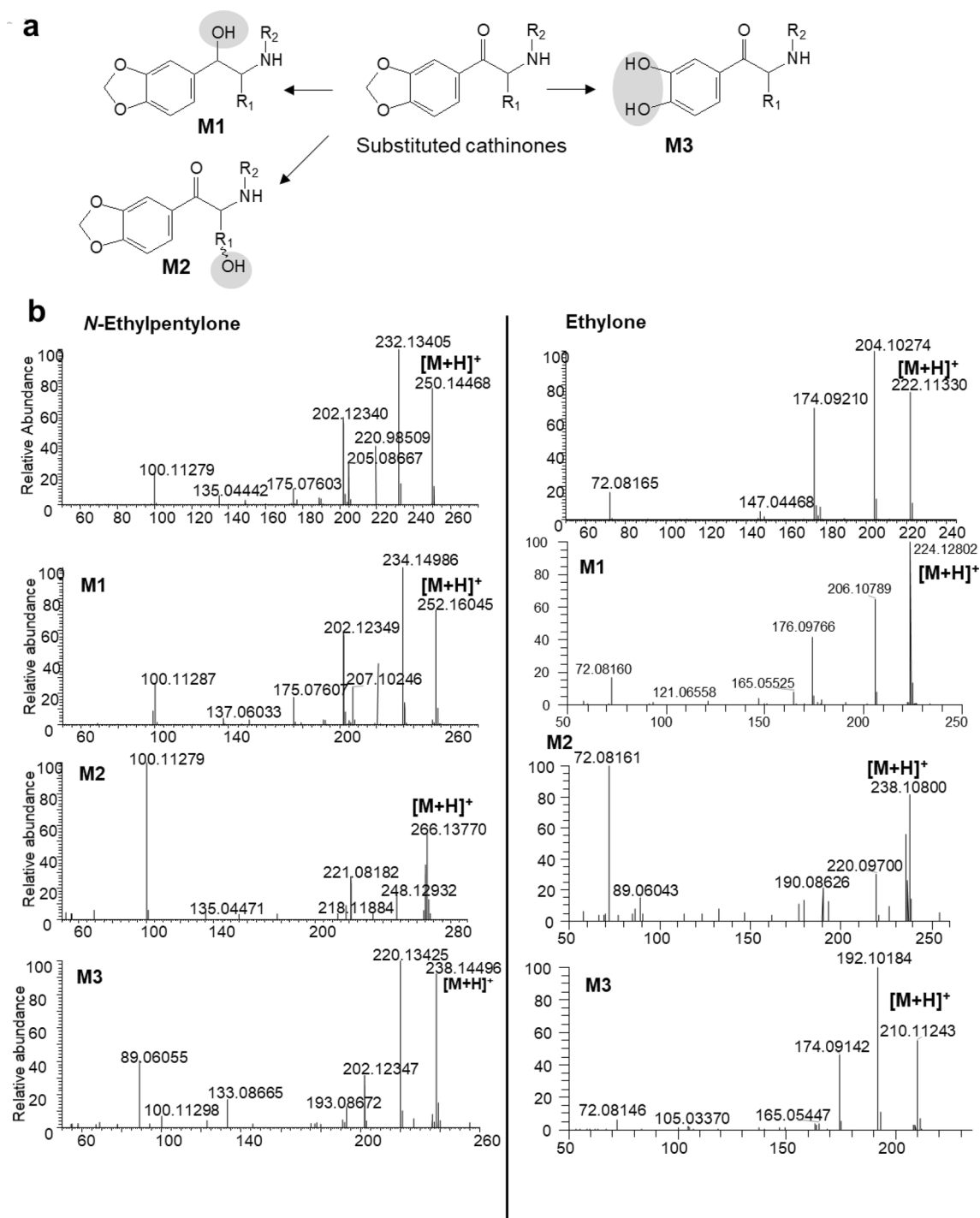


Fig. 3 **a** Proposed *in vivo* metabolic pathways for substituted cathinones (ethylone R_1 : CH_3 , R_2 : C_2H_5 ; *N*-ethylpentylone R_1 : C_3H_8 , R_2 : C_2H_5) in zebrafish; metabolic reaction highlighted in grey in each

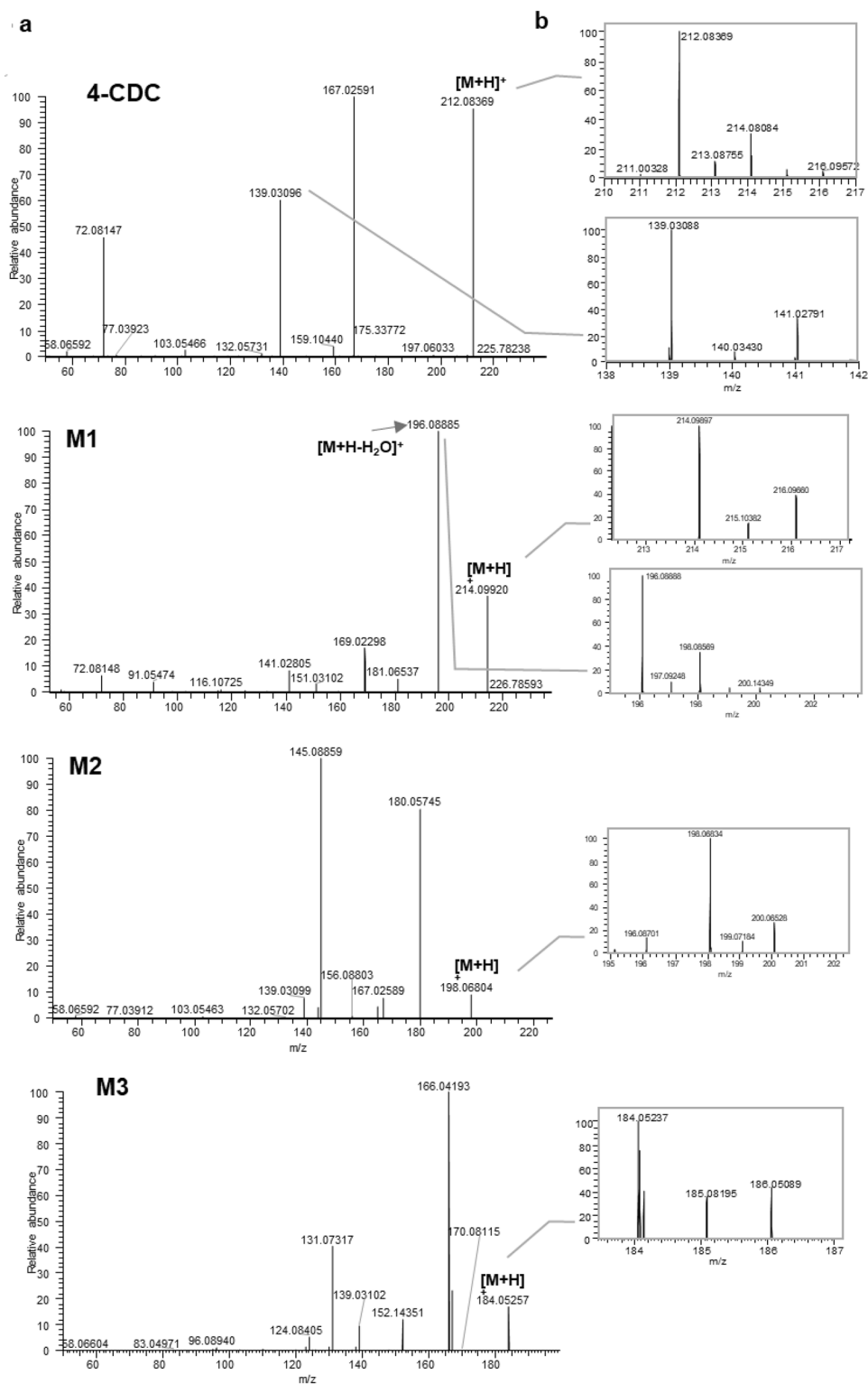
structure. **b** HR-MS/MS spectra (ESI(+)) of ethylone and its metabolite in the right column and *N*-ethylpentylone and its metabolites in the left column

this is an evidence of the degree of dissemination of synthetic drugs around the world.

In addition to the lack of traceability of drugs production, the possibility of adulteration or dilution with other substances (e.g. caffeine, ketamine, talcum) to mimic or

modify the drugs' effect, cheapening its cost needed to be considered [29]. Thus, considering the composition of this illicit material can vary significantly, with clear impact in the metabolism results, a comprehensive characterization, e.g., GC-MS, ^1H NMR and IR was conducted to verify the

Fig. 4 **a** HR-MS/MS spectra of 4-CDC and its metabolites. **b** Isotopic patterns



molecular identification of the substances. All cationones involved that were properly characterized presented high levels of purity. In other words, it was not observed any interferences and adulterants considering these methods' sensitivity.

The putative metabolites were initially inferred by the knowledge of the classical CYP-mediated metabolic pathways for xenobiotics. Then, the exact masses of these metabolite candidates were obtained using the software Xcalibur 3.0 (Thermo Fisher Scientific). Multiple MS experiments

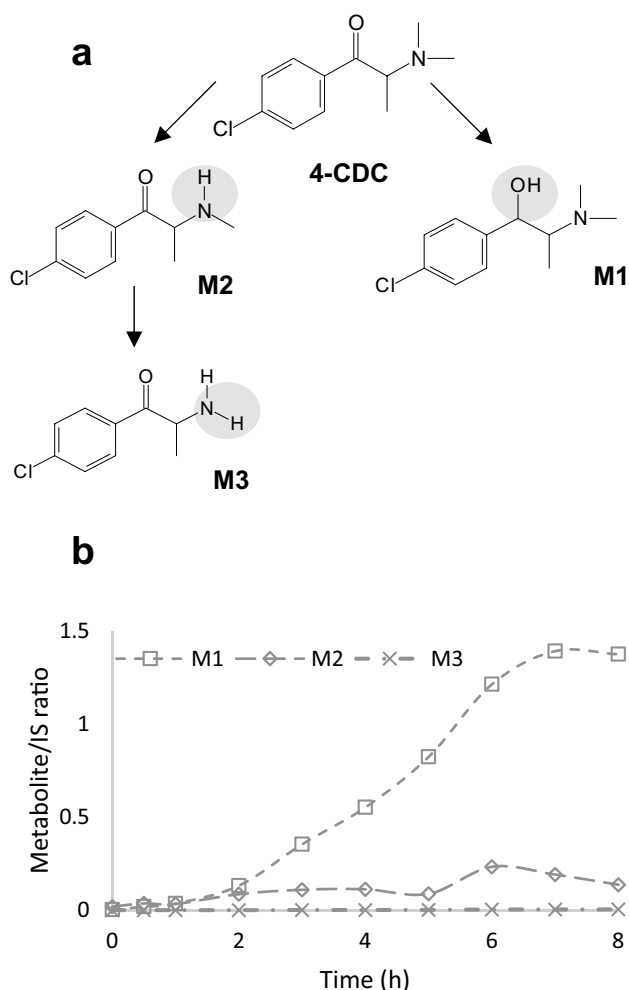


Fig. 5 **a** Proposed metabolic pathways for 4-CDC metabolic reaction highlighted in grey in each structure. **b** Accumulation curve of 4-CDC metabolites. *IS* internal standard (7-propyltheophylline)

ran in parallel, allowing the acquisition of a huge amount of data. The exact mass ion chromatograms from full-scan mode were extracted evidencing the presence, or not, of each putative metabolite. Comparison of the chromatograms obtained from the test tanks and the positive and negative control tanks were used for this goal. The HR-MS/MS spectra were useful to obtain the fragment elemental composition and thus to infer structures by comparing with data from the literature. The HR-MS/MS (full-scan/MS²) fragmentation experiments were conducted through the creation of an inclusion list with the expected $[M+H]^+$ of its supposed metabolites. These data-independent acquisition experiments already demonstrated the improvement of the method sensibility [2]. This total MS acquisition strategy enables the detection of the predicted m/z relative to the metabolites inferred based on the classical metabolism information, meanwhile it allows the acquisition of all analytical information, creating the perspective of a comprehensive

non-target method. If an unpredicted metabolite is not immediately observed, the raw file data can be reevaluated a posteriori to find a new metabolic pathway. In this way, chemical structures of the putative metabolites were postulated by interpretation of the mass shifts in the HR-MS/MS spectrum in relation of the parent compound and in accordance with previously published data.

All metabolites described herein were observed in the three replicates and not observed either in the positive or negative control (data not shown).

The study of the *N*-pyrrolidine cathinone, α -PVP, in ZWT yielded five metabolites. *N,N*-bis-dealkylation (**M1**), hydroxylation in the pyrrolidine ring (**M2**), β -keto moiety reduction (**M4**), β -keto reduction plus hydroxylation in the pyrrolidine ring (**M3**) and oxidation product at the 2-position of the pyrrolidine ring (**M5**) were the main metabolic pathways found in ZWT (Table 1, Fig. 2). However, in the present study only one chromatography peak was observed for 1-hydroxy- α -PVP (**M4**), although this metabolite was reported a mixture of diastereomers in human urine [21]. The authors found huge discrepancies among these isomers' concentrations, which were attributed to stereospecific affinities of *R*- and *S*- α -PVP for the enzyme responsible for the metabolization. Thus, the chromatographic conditions employed in our study may have to be optimized to figure them out if the ZWT is able to produce both isomers.

Considering that the metabolites are continually eliminated by the fish in the water, it is reasonable to expect a cumulative profile in the water tank. Of course, given that the newly formed metabolites are available to interact continually with the zebrafish enzymatic machinery, i.e., being reabsorbed, metabolized and excreted, different metabolites could show a less/more significant concentration increase in the tank. This behavior is commonly observed in *in vitro* systems, where the excretion step, using the human model analogy, could not be reproduced [30]. Hence, kinetic inferences using the ZWT should be carefully made, being hard to extrapolate the data to perform comparisons with other *in vivo* models. Anyway, the metabolite concentration increment over time is an important complementary tool to evaluate the ability of the zebrafish to metabolize xenobiotics.

For *N*-ethylpentylone and ethylone, 6 metabolites were found in ZWT (Table 2, Fig. 3a). Reduction of the keto moiety (**M1**), hydroxylation (**M2**) and demethylenation (**M3**) were also observed in the human biological fluids studied [31, 32]. Although phase II glucosylated metabolites were already described for α -PVP and ethylone in humans [21, 33], such conjugated metabolites were not observed in this study. It is due to the incubation step with β -glucuronidase from *E. coli* adopted in the experimental design. In theory, if formed by the model, the phase II metabolites could be detected based on the 10 μ L of *in nature* aquarium water was added to the final extract just

before the injection in LC–HR–MS system [1]. Nevertheless, in this study, the lack of detection of such metabolites could be associated to the small amounts in the samples. A dedicated study must be conducted with ZWT to evaluate the phase II metabolites for synthetic cathinones.

The metabolism of 4-CDC in humans or other in vivo or even in in vitro models have not yet been reported to our knowledge. Therefore, considering the structural similarity with other cathinones already studied [34], the metabolites were hypothesized, and dealkylation, β -ketone-reduction and hydroxylation could be demonstrated as metabolic pathways of 4-CDC. Based on the findings for 4-chloro-*N,N*-diethylcathinone, which suggested that the product of carbonyl reduction was the most intense metabolite observed in human biosamples (plasma and urine) and S9 fraction incubation experiments (unpublished observation), it is reasonable to suggest the keto reduction metabolite (**M1**), the main metabolite observed in ZWT, as a target metabolite for forensic analysis of 4-CDC also in humans.

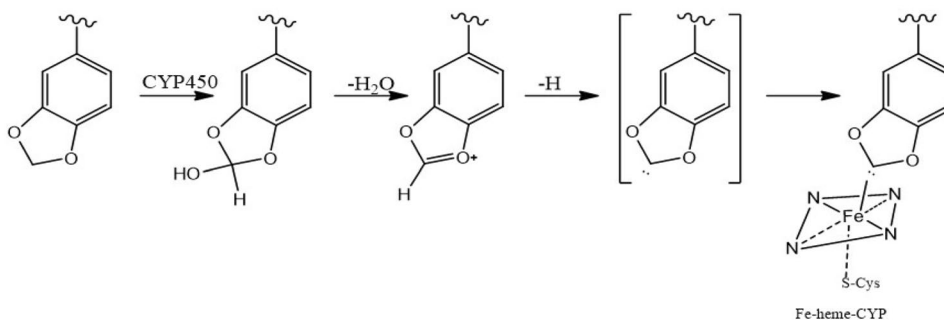
Pedersen et al. [27] reported that CYP2D6 was shown to be the primary enzyme that metabolizes methylone, with minor contributions from CYP1A2, CYP2B6, and CYP2C19. The authors also showed a time-dependent loss of CYP2D6 activity when the enzyme was preincubated with methylone. Indeed, the loss of activity reached a maximum rate of inactivation at high methylone concentrations, suggesting that methylone is a mechanism-based inhibitor of CYP2D6. Methylone showed inhibitory potential similar to clinically important inhibitors such as quinidine [27]. In fact, CYP enzymes oxidize aryl and alkyl methylenedioxy compounds to species that coordinate tightly to their heme iron atom. This is likely via the interaction of a carbene formed from the methylene group and the iron atom of the heme moiety (Fig. 6). Paroxetine is an example of a drug that inhibits P450 by this mechanism [35].

According to Goldstone et al. [36], the zebrafish would not have CYP orthologous to human CYP 2D6. Although no ortholog of human CYP2D6 has been found in the fish, which could initially explain why we did not observe the metabolism in this model, zebrafish has been described to metabolize dextromethorphan, a substrate of human

CYP2D6, to dextrorphan in addition to 3-methoxymorphinan [37]. This indicates that not having a human CYP ortholog in zebrafish does not necessarily mean that there will be no biotransformation of drugs. Considering different β -keto designed drugs metabolites (e.g., ethylone and *N*-ethylpentylone), it is possible that methylone exhibits a behavior on CYP isoenzymes for zebrafish, which is similar to the action of methylone on human CYP2D6 [37, 38]. Our findings for α -PVP metabolism corroborate our hypothesis because CYP2D6 has been described as the only responsible for the formation of **M3** and **M4** metabolites of α -PVP. In addition, this CYP is the majorly responsible for the formation of α -PVP **M1**. As mentioned earlier, despite that this enzyme has no direct ortholog in zebrafish [26], it is reasonable that other CYP enzymes presented in zebrafish liver have a similar functionality to CYP2D6 in carrying out the oxidative metabolism of this molecule. However, further studies should be performed to evaluate which zebrafish CYPs are involved in metabolism of this substance.

The reference standards of cathinone metabolites collected from ZWT experiment seem very promising, because many of them are not commercially available. The outcome of ZWT, basically water, is a much cleaner matrix than any biological one, which can help in the identification of new metabolites. In addition, there is no limit on the outcome of the experiment. Theoretically, it is possible to scale up the experiment, working with liters of water. The outcome material replete with metabolites could be concentrated and used in analytical batches as positive quality controls. Finally, it is possible to run a validation protocol to evaluate classical analytical merits such as selectivity/specificity and inter/intra-assay precision since blank samples from a biologic fluid of choice could be spiked with a concentrated solution of the reference standards collected via the ZWT experiments.

Fig. 6 Cytochrome P450 inhibition mechanism proposed for methylone



Conclusions

In the present study, the utility of ZWT approach for the phase I metabolism assessment was demonstrated using *N*-ethylpentylone, ethylone, methylone, α -PVP and 4-CDC as model drugs. The main metabolites described in the literature for *N*-ethylpentylone, ethylone, α -PVP and 4-CDC were observed through the ZWT model reinforcing its capacity to produce the same metabolites as observed in the human model. Especially for 4-CDC, the metabolism of which has not yet been investigated in humans, three metabolites were detected, and the reduction on the keto moiety product was suggested as the main metabolic pathway. Methylone seems to be a potent CYP inhibitor in zebrafish, although more experiments are needed to better evaluate this issue. *N*-Ethylpentylone was used as a pilot experiment for reference standard collection of its metabolites, demonstrating the viability of the zebrafish model to produce such material with high throughput, low cost, without exposing human volunteers to drugs. Based on the results here presented, zebrafish have been indicated as an excellent model to study the metabolism of synthetic cathinones.

Acknowledgements This work was supported by CAPES and by an institutional covenants with the Civil Police of Rio de Janeiro State (PCERJ/ICCE) and the National Institute of Criminalistics of the Brazilian Federal Police (SEPLAB).

Compliance with ethical standards

Conflict of interest The authors declare that they have no conflicts of interest associated with the present work.

Ethical approval This study was approved by the Ethics Committee on the Use of Animals of the Federal University of Rio de Janeiro through protocol number 065/19.

Open Access This article is licensed under a Creative Commons Attribution 4.0 International License, which permits use, sharing, adaptation, distribution and reproduction in any medium or format, as long as you give appropriate credit to the original author(s) and the source, provide a link to the Creative Commons licence, and indicate if changes were made. The images or other third party material in this article are included in the article's Creative Commons licence, unless indicated otherwise in a credit line to the material. If material is not included in the article's Creative Commons licence and your intended use is not permitted by statutory regulation or exceeds the permitted use, you will need to obtain permission directly from the copyright holder. To view a copy of this licence, visit <http://creativecommons.org/licenses/by/4.0/>.


References

- Sardela VF, Martucci MEP, de Araújo ALD, Leal EC, Oliveira DS, Carneiro GRA, Deventer K, Van Eenoo P, Pereira HMG, Aquino Neto FR (2018) Comprehensive analysis by liquid chromatography-Q-Orbitrap mass spectrometry: fast screening of peptides and organic molecules. *J Mass Spectrom* 53:476–503. <https://doi.org/10.1002/jms.4077>
- UNODC (2018) World drug report 2018. Booklet 3. Analysis of drug markets: opiates, cocaine, cannabis, synthetic drugs. http://www.unodc.org/wdr2018/prelaunch/WDR18_Booklet_3_DRUG_MARKETS.pdf. Accessed 3 June 2020
- Błażewicz A, Bednarek E, Popławska M, Olech N, Sitkowski J, Kozerski L (2019) Identification and structural characterization of synthetic cathinones: *N*-propylcathinone, 2,4-dimethylmethcathinone, 2,4-dimethylethcathinone, 2,4-dimethyl- α -pyrrolidinopropiophenone, 4-bromo- α -pyrrolidinopropiophenone, 1-(2,3-dihydro-1*H*-inden-5-yl)-2-(pyrrolidin-1-yl)hexan-1-one and 2,4-dimethylisocathinone. *Forensic Toxicol* 37:288–307. <https://doi.org/10.1007/s11419-018-00463-w> (open access article)
- Cheng W-C, Wong W-C (2019) Forensic drug analysis of chloro-*N,N*-dimethylcathinone (CDC) and chloroethcathinone (CEC): identification of 4-CDC and 4-CEC in drug seizures and differentiation from their ring-substituted positional isomers. *Forensic Sci Int* 298:268–277. <https://doi.org/10.1016/j.forsciint.2019.03.002>
- Gerostamoulos D, Elliott S, Walls HC, Peters FT, Lynch M, Drummer OH (2016) To measure or not to measure? That is the NPS question. *J Anal Toxicol* 40:318–320. <https://doi.org/10.1093/jat/bkw013> (open access article)
- Valente MJ, de Pinho PG, de Lourdes Bastos M, Carvalho F, Carvalho M (2014) Khat and synthetic cathinones: a review. *Arch Toxicol* 88:15–45. <https://doi.org/10.1007/s00204-013-1163-9>
- Prosser JM, Nelson LS (2012) The toxicology of bath salts: a review of synthetic cathinones. *J Med Toxicol* 8:33–42. <https://doi.org/10.1007/s13181-011-0193-z> (open access article)
- UNODC (2019) World drug report 2019. <http://www.unodc.org/wdr2019/>. Accessed 3 Jun 2020
- Saito T, Namera A, Osawa M, Aoki H, Inokuchi S (2013) SPME-GC-MS analysis of α -pyrrolidinovalerophenone in blood in a fatal poisoning case. *Forensic Toxicol* 31:328–332. <https://doi.org/10.1007/s11419-013-0183-8>
- Grafinger KE, Wilke A, König S, Weinmann W (2019) Investigating the ability of the microbial model *Cunninghamella elegans* for the metabolism of synthetic tryptamines. *Drug Test Anal* 11:721–729. <https://doi.org/10.1002/dta.2544>
- Schaefer N, Wojtyniak J-G, Kettner M, Schlote J, Laschke MW, Ewald AH, Lehr T, Menger MD, Maurer HH, Schmidt PH (2016) Pharmacokinetics of (synthetic) cannabinoids in pigs and their relevance for clinical and forensic toxicology. *Toxicol Lett* 253:7–16. <https://doi.org/10.1016/j.toxlet.2016.04.021>
- Appolonova SA, Palacio C, Shestakova KM, Mesonzhnik NV, Roman AB, Kuznetsov M, Markin PA, Bochkareva NL, Burmykin D, Ovcharov M, Musile G, Tagliaro F, Savchuk SA (2020) In vivo and in vitro metabolism of the novel synthetic cannabinoid 5F-APINAC. *Forensic Toxicol* 38:160–171. <https://doi.org/10.1007/s11419-019-00503-z>
- Sardela VF, de Sousa Anselmo C, da Costa Nunes IK, Carneiro GRA, dos Santos GRC, de Carvalho AR, de Jesus LaBanca B, Oliveira DS, Ribeiro WD, de Araújo ALD, Padilha MC, de Lima CKF, de Souza VP, de Aquino Neto FR, Pereira HMG (2018) Zebrafish (*Danio rerio*) water tank model for the investigation of drug metabolism: progress, outlook, and challenges. *Drug Test Anal* 10:1657–1669. <https://doi.org/10.1002/dta.2523>
- Streisinger G, Walker C, Dower N, Knauber D, Singer F (1981) Production of clones of homozygous diploid zebrafish (*Brachydanio rerio*). *Nature* 291:293–296. <https://doi.org/10.1038/291293a0>
- de Souza Anselmo C, Sardela VF, de Souza VP, Pereira HMG (2018) Zebrafish (*Danio rerio*): a valuable tool for predict the

- metabolism of xenobiotics in humans? *Comp Biochem Physiol C* 212:34–46. <https://doi.org/10.1016/j.cbpc.2018.06.005>
16. Matos RR, Martucci MEP, de Anselmo CS, Aquino Neto FR, Pereira HMG, Sardela VF (2020) Pharmacokinetic study of xylazine in a zebrafish water tank, a human-like surrogate, by liquid chromatography Q-Orbitrap mass spectrometry. *Forensic Toxicol* 38:108–121. <https://doi.org/10.1007/s11419-019-00493-y>
 17. De Souza Anselmo C, Sardela VF, Matias BF, De Carvalho AR, De Sousa VP, Pereira HMG, De Aquino Neto FR (2017) Is zebrafish (*Danio rerio*) a tool for human-like metabolism study? *Drug Test Anal* 9:1685–1694. <https://doi.org/10.1002/dta.2318> (**open access article**)
 18. Sardela VF, Sardela PDO, Lisboa RR, Matias BF, Anselmo CS, de Carvalho AR, Nunes IKC, Padilha MC, de Aquino Neto FR, Pereira HMG (2020) Comprehensive zebrafish water tank experiment for metabolic studies of testolactone. *Zebrafish* 17:104–111. <https://doi.org/10.1089/zeb.2019.1791>
 19. Xu DQ, Dai Y, Zhang WF, Wang Y-Y, Zhang Y, Wang J-F, Zhao Q-L, Li X (2020) Rapid identification of MDMA-CHMINACA metabolites using zebrafish and human liver microsomes as the biotransformation system by LC-QE-HF-MS. *J Anal Toxicol* 5:8. <https://doi.org/10.1093/jat/bkaa001> (**Online ahead of print**)
 20. Negreira N, Erratico C, Kosjek T, van Nuijs ALN, Heath E, Neels H, Covaci A (2015) In vitro phase I and phase II metabolism of α -pyrrolidinovalerophenone (α -PVP), methylenedioxypropylvalerone (MDPV) and methedrone by human liver microsomes and human liver cytosol. *Anal Bioanal Chem* 407:5803–5816. <https://doi.org/10.1007/s00216-015-8763-6>
 21. Shima N, Katagi M, Kamata H, Matsuta S, Sasaki K, Kamata T, Nishioka H, Miki A, Tatsuno M, Zaitsu K, Ishii A, Sato T, Tsuchihashi H, Suzuki K (2014) Metabolism of the newly encountered designer drug α -pyrrolidinovalerophenone in humans: identification and quantitation of urinary metabolites. *Forensic Toxicol* 32:59–67. <https://doi.org/10.1007/s11419-013-0202-9>
 22. Qian Z, Jia W, Li T, Hua Z, Liu C (2017) Identification of five pyrrolidinyl substituted cathinones and the collision-induced dissociation of electrospray-generated pyrrolidinyl substituted cathinones. *Drug Test Anal* 9:778–787. <https://doi.org/10.1002/dta.2035>
 23. Tyrkkö E, Plander A, Ketola RA, Ojanperä I (2013) In silico and in vitro metabolism studies support identification of designer drugs in human urine by liquid chromatography/quadrupole-time-of-flight mass spectrometry. *Anal Bioanal Chem* 405:6697–6709. <https://doi.org/10.1007/s00216-013-7137-1>
 24. Niessen WM, Correa RA (2017) Interpretation of MS-MS mass spectra of drugs and pesticides. Wiley, Hoboken
 25. Kamata HT, Shima N, Zaitsu K, Kamata T, Nishikawa M, Katagi M, Miki A, Tsuchihashi H (2007) Simultaneous analysis of new designer drug, methylone, and its metabolites in urine by gas chromatography-mass spectrometry and liquid chromatography-electrospray ionization mass spectrometry. *Jpn J Forensic Sci Tech* 12:97–106. <https://doi.org/10.3408/jafst.12.97>
 26. Kamata HT, Shima N, Zaitsu K, Kamata T, Miki A, Nishikawa M, Katagi M, Tsuchihashi H (2006) Metabolism of the recently encountered designer drug, methylone, in humans and rats. *Xenobiotica* 36:709–723. <https://doi.org/10.1080/00498250600780191>
 27. Pedersen AJ, Petersen TH, Linnert K (2013) In vitro metabolism and pharmacokinetic studies on methylone. *Drug Metab Dispos* 41:1247–1255. <https://doi.org/10.1124/dmd.112.050880>
 28. WHO (2018) Critical review report: *N*-ethylnorpentylone. <https://www.who.int/medicines/access/controlled-substances/N-Ethyl-norpentylone.pdf>. Accessed 31 May 2020
 29. Togni LR, Lanaro R, Resende RR, Costa JL (2015) The variability of ecstasy tablets composition in Brazil. *J Forensic Sci* 60:147–151. <https://doi.org/10.1111/1556-4029.12584>
 30. De Brabanter N, Esposito S, Tudela E, Lootens L, Meuleman P, Leroux-Roels G, Deventer K, Van Eenoo P (2013) In vivo and in vitro metabolism of the synthetic cannabinoid JWH-200. *Rapid Commun Mass Spectrom* 27:2115–2126. <https://doi.org/10.1002/rcm.6673>
 31. Krotulski AJ, Papsun DM, De Martinis BS, Mohr ALA, Logan BK (2018) *N*-Ethylpentylone (ephylone) intoxications: quantitative confirmation and metabolite identification in authentic human biological specimens. *J Anal Toxicol* 42:467–475. <https://doi.org/10.1093/jat/bky025> (**open access article**)
 32. Zawadzki M, Nowak K, Szpot P (2020) Fatal intoxication with *N*-ethylpentylone: a case report and method for determining *N*-ethylpentylone in biological material. *Forensic Toxicol* 38:255–263. <https://doi.org/10.1007/s11419-019-00483-0> (**open access article**)
 33. Zaitsu K, Katagi M, Kamata HT, Kamata T, Shima N, Miki A, Tsuchihashi H, Mori Y (2009) Determination of the metabolites of the new designer drugs bk-MBDB and bk-MDEA in human urine. *Forensic Sci Int* 188:131–139. <https://doi.org/10.1016/j.forsciint.2009.04.001>
 34. Wagemann L, Manier SK, Eckstein N, Maurer HH, Meyer MR (2020) Toxicokinetic studies of the four new psychoactive substances 4-chloroethcathinone, *N*-ethylnorpentylone, *N*-ethylhexedrone, and 4-fluoro- α -pyrrolidinohexiophenone. *Forensic Toxicol* 38:59–69. <https://doi.org/10.1007/s11419-019-00487-w>
 35. Ashby J, Elliott BM (1984) 1,3-Benzodioxole derivative. In: Katritzky AR, Rees CW (eds) *Comprehensive heterocyclic chemistry*. Pergamon, Oxford, pp 111–141
 36. Goldstone JV, Kubota A, Zanette J, Parente T, Jönsson ME, Nelson DR, Stegeman JJ (2010) Identification and developmental expression of the full complement of cytochrome P450 genes in zebrafish. *BMC Genom* 11:643. <https://doi.org/10.1186/1471-2164-11-643>
 37. Saad M, Matheussen A, Bijttebier S, Verbueken E, Pype C, Casteleyn C, Van Ginneken C, Apers S, Maes L, Cos P, Van Cruichten S (2017) In vitro CYP-mediated drug metabolism in the zebrafish (embryo) using human reference compounds. *Toxicol In Vitro* 42:329–336. <https://doi.org/10.1016/j.tiv.2017.05.009>
 38. Jackson KD, Durandis R, Vergne MJ (2018) Role of cytochrome P450 enzymes in the metabolic activation of tyrosine kinase inhibitors. *Int J Mol Sci* 19:2367. <https://doi.org/10.3390/ijms19082367> (**open access article**)

Publisher's Note Springer Nature remains neutral with regard to jurisdictional claims in published maps and institutional affiliations.

Affiliations

Estefany Prado¹ · Rebecca Rodrigues Matos¹ · Geovana Maria de Lima Gomes¹ · Clarisse Baptista Lima de Sá¹ · Isabelle Karine da Costa Nunes¹ · Carina de Souza Anselmo¹ · Adriana Sousa de Oliveira² · Luciana Silva do Amaral Cohen² · Denilson Soares de Siqueira² · Marco Antônio Martins de Oliveira^{2,4} · João Carlos Laboissiere Ambrosio³ · Gabriela Vanini Costa^{1,5} · Francisco Radler de Aquino Neto¹ · Monica Costa Padilha¹ · Henrique Marcelo Gualberto Pereira¹ 

¹ Instituto de Química, LBCD-LADETEC, Universidade Federal do Rio de Janeiro, Avenida Horácio Macedo, no. 1281, Polo de Química, bloco C, Cidade Universitária, Rio de Janeiro, RJ 21941-598, Brazil

² Departamento Geral de Polícia Técnico Científica do Rio de Janeiro, Instituto de Criminalística Carlos Éboli, (ICCE/DGPTC/PCERJ), Rua Pedro I, 28-Centro, Rio de Janeiro, RJ 20060-050, Brazil

³ Departamento de Polícia Federal, Instituto Nacional de Criminalística, Spo-Quadra 07 Lote 23, Estr. St. Polícia Militar, Asa Sul, Brasília, DF 70610-200, Brazil

⁴ Departamento de Química Analítica, Instituto de Química, Universidade Federal Fluminense, Outeiro de São João Batista s/n, Campus do Valonguinho, Niterói, RJ 24020-150, Brazil

⁵ Instituto de Química, NAF-LADETEC, Universidade Federal do Rio de Janeiro, Avenida Horácio Macedo, no. 1281, Polo de Química, bloco C, Cidade Universitária, Rio de Janeiro, RJ 21941-98, Brazil